STOCHASTIC ANALYSIS OF PRE- AND POST-EXPOSURE PROPHYLAXIS AGAINST HIV INFECTION*

JESSICA M. CONWAY†, BERNHARD P. KONRAD‡, AND DANIEL COOMBS‡

Abstract. The events that occur following HIV exposure, preceding any detectable infection are difficult to study experimentally. However, there is considerable evidence that these events can be influenced by the action of antiretroviral drugs, taken either as pre- or post- exposure prophylaxis (PrEP and PEP, respectively). We present simple theoretical models of HIV dynamics immediately following exposure, and apply these models to understanding how drug prophylaxis can act to reduce the risk of infection. Because HIV infection following exposure is a relatively rare event, we work with stochastic models which we base on continuous-time branching processes, allowing us to compute the risk of infection under different scenarios. We are able to obtain analytical solutions for viral extinction probabilities, allowing us to avoid extensive computer simulations. We predict in the case of PrEP that reverse transcriptase inhibitors should be somewhat more effective than protease inhibitors and also that single drugs should be nearly as effective as a combination approach. We then model viral dynamics under PEP and find that fast initiation of therapy is essential for risk reduction. However, we predict that a two-week PEP regimen would be nearly as effective as the current recommendation of four weeks of therapy. Our work provides a coherent platform for studying the early dynamics of HIV and indicates possible directions for experimental and theoretical work.

Key words. HIV viral dynamics, branching process, pre-exposure prophylaxis, post-exposure prophylaxis, HIV prevention

AMS subject classifications. 92C50, 62C50, 60J85

1. Introduction.

The events of the first few hours to days immediately following exposure to HIV are of critical importance in determining whether infection will occur. However, it is very difficult to study these events in human patients or animal models, because the numbers of viruses and infected cells at this stage are extremely low. A brief summary of some key points of our knowledge is as follows: First, typical sexual or blood exposure to virus rarely leads to infection, with human transmission probabilities estimated in the range of $0.1 - 1\%$ per act [26]. Second, phylogenetic analysis of the viral strains dominant in chronically infected individuals points to a strong evolutionary bottleneck during early infection, with many infections arising from a single founder strain [22]. Finally, it appears that there is a narrow window of opportunity for post-exposure drug treatment (or potentially, an immune response) to help prevent infection [6, 26].

Indeed, post-exposure prophylaxis (PEP) has been used successfully for two decades to prevent occupational infection. The guidelines for PEP recommend that extremely high doses of antiretroviral therapy (ART) are taken within 72 hours of exposure, and continue for 28 days. PEP has been found to be an effective treatment, reducing the rate of infection following an occupational needlestick exposure

*This work was supported by the Natural Science and Engineering Research Council of Canada and by the Canadian Institutes of Health Research [funding reference number HFE-105370 to JMC; Grant No. HET 85520], the Pacific Institute for Mathematical Sciences through the International Graduate Training Centre in Mathematical Biology, and was enabled by the use of computing resources provided by WestGrid and Compute/Calcul Canada. We thank Denis Conway, Rafael Meza, Michael Gilchrist, Alejandra Herrera for useful discussions, and several anonymous reviewers for helpful feedback.

†T-6, Theoretical Biology and Biophysics, MS-K710, Los Alamos National Laboratory, Los Alamos, NM, 87545

‡Department of Mathematics and Institute of Applied Mathematics, University of British Columbia, 1984 Mathematics Road, Vancouver, BC V6T 1Z2, Canada

by approximately 80% [6, 26]. For this reason, non-occupational PEP therapy following sexual or other exposure has been studied, but with inconclusive results regarding clinical effectiveness [39, 5]. In a similar vein, recent clinical trials of pre-exposure prophylaxis (PrEP) have shown variable success in reducing new infections in high-risk populations. PrEP is the HIV prevention measure in which anti-retroviral treatments (ARTs) are taken in advance of possible exposure, and reductions in incidence in the range of $40 - 80\%$ have been reported in some studies [13, 2, 43]. The FDA recently approved PrEP for high-risk groups and it seems likely that larger studies and broader application of PrEP will be forthcoming.

In this paper we present new mathematical models of early HIV infection and indicate how our results may inform the use of PrEP and PEP therapies. Since we are studying the dynamics of very few infected cells and very few virions, we must apply fully stochastic models, extending recent theoretical studies of HIV infection by ourselves [9] and others [34], which themselves build on an earlier literature [46, 28, 31, 19]. We distinguish the present work from earlier studies by avoiding computer simulation of the models, in favour of an analytical formulation, and by our focus on models designed to give information on different aspects of PrEP and PEP.

We begin the Methods section by describing two models (one simple and one more complex) that aim to describe early HIV infection. By expressing these models as continuous-time branching processes, we are able to calculate the probability of infection by a single founder virus. This probability depends on the parameters of the model, and includes the effects of any drug treatment. In the case of PrEP, we can reduce the probability of infection to a simple analytic expression, but for PEP, we have to use numerical integration. In the Results section, we predict the effects of different prophylaxis regimens (which class of drugs, when and for how long) using the different models. For clarity, we have divided the results into four subsections: basic results on inoculum size and number of successful viral lineages, PrEP results, PEP results, and an examination of an alternative model for viral production. We conclude with a discussion of implications of the results and some ideas for possible future work.

We want to make especially clear that all our results were obtained either from analytical formulae (results with no treatment or PrEP) or numerical integration of ODEs to obtain certain probability distributions (PEP). We present no simulations and remarkably, this paper cites Gillespie exactly once [12].

2. Methods.

Stochastic models of early infection. We will present results from two models of early HIV infection: a simple model that captures several essential features of early infection, and a more complex model that includes dendritic cell capture and transport of HIV to the lymphoid tissues. In this section, we present the details of both models, and show how we obtain analytical results from the simpler model. The analysis of the more complex model is essentially identical, but the mathematical formulae are (much) longer.

Simple model of early HIV infection. Our basic model of early HIV infection is presented schematically in Fig. 2.1a. There are four compartments: replication-competent and -incompetent virus V and W respectively, and infected cells in the eclipse phase (not producing virus) T_1^* and productive phase T_2^*. Viruses are cleared at rate c and infect new cells at rate kT, where k represents a mass-action infectivity, and T represents the local number of target cells. In contrast to standard differential equation models of HIV infection, T can be held fixed because very few cells are

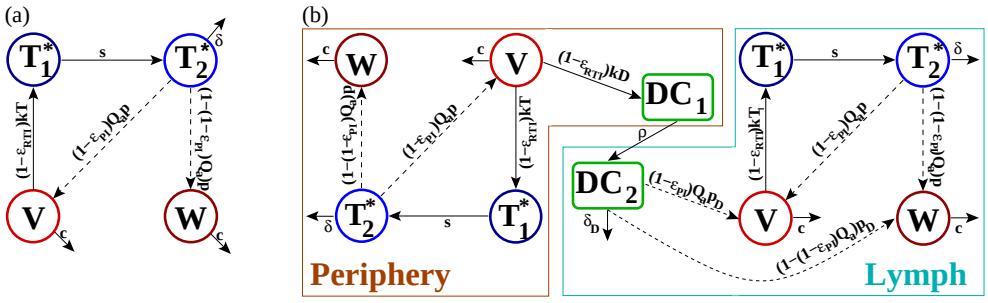

FIG. 2.1. ***Model schematics***. *(a) Simple, one-compartment model of early HIV infection. (b) Two-compartment model with transport.*

infected at the stage of infection we are considering. Newly infected cells pass from the eclipse phase to the productive phase at constant rate s, providing a mean delay of magnitude $1/s$ between infection and viral production. Productively infected cells are lost at rate δ and produce virus at rate p, but only a fraction Q_a of these viruses are replication-competent. Drugs are included in the form of protease inhibitors (PIs) and reverse transcriptase inhibitors (RTIs). PIs interfere with the maturation of new viruses, decreasing Q_a and thereby causing an increase in the fraction of produced replication-incompetent virus, with efficacy $\varepsilon_{\mathrm{PI}}$. RTIs prevent infection of new cells with efficacy $\varepsilon_{\mathrm{RTI}}$. The eclipse phase of the infected cells is explicitly included in our model to capture separate effects of these drugs with regards to timing of PEP.

In a recent paper, Pearson et al. [34] distinguished early infection models with continuous viral production (as described above) from bursting models, where an infected cell releases all its progeny virions at the end of its lifetime. What happens in reality remains unclear. We will use both models of production in this paper, presenting continuous production model results first.

Two-compartment model with viral transport . The simple model neglects different cell types and transport dynamics thought to be important in the initiation of HIV infection. In particular, it does not capture the hypothesis that successful HIV infection is promoted by dendritic cells (DCs) that take up virus in the periphery, either via infection (cis-infection) or adhesion to the DC surface/assimilation into endosomes (trans-infection) and carry HIV to the lymphoid tissue, where there is a high density of T cells [15]. In the lymphoid tissue, DC/T cell interactions are thought to facilitate rapid infection [51].

We therefore present an extended model that explicitly includes DCs and a lymphoid tissue compartment (Fig. 2.1b). In this model, the target cell - viral dynamics of the peripheral compartment, which are taken to be the same as in the simple model, are coupled to the lymphoid tissue by mobile DCs. The peripheral compartment could represent the blood (e.g. for needlestick exposure) or the genital mucosa (in the case of sexual exposure). We assume that DCs become infected at rate kD in the periphery and travel to the lymph (with mean transit time $1/\rho$). The DC is removed after spending a mean time $1/\delta_D$ in the lymph, where it produces virions at rate p_D. Infection and production rates of DCs are modulated by anti-retroviral drugs in the same way as in other target cells. We also examine the implications of reduced drug efficacy in the lymphoid compartment. Viruses released by DCs in the lymph are then able to infect the larger population of T cells at that location. For simplicity, we do not explicitly model DC-T cell binding interactions or trans-infection of DCs.

In the following, we will refer to this model as the "two-compartment model" and to the simple model as the "one-compartment model."

Parameters. The baseline parameters used for our results are given in Table 2.1. The parameters governing the early stages of HIV infection are likely to differ from

TABLE 2.1
Model Parameters.

Parameter	Description	Estimate
δ	Death rate of productively infected cells	1 day^{-1}
s	Rate at which infected target cells leave the eclipse phase	1 day^{-1}
p	Virion production rate	20000 day^{-1}
c	Virion clearance rate	23 day^{-1}
Q_c	Replication-competent virion fraction in exposure inoculum	10^{-3}
Q_a	Replication-competent virion fraction	10^{-2}, varied
$\varepsilon_{\mathrm{RTI}}$	RTI drug efficacy	0.9, varied
$\varepsilon_{\mathrm{PI}}$	PI drug efficacy	0.9, varied

their counterparts in chronic HIV infection. However, since there are few reports of these parameters in the earliest stages of infection, we mostly use chronic infection parameters as first approximations. We take the mean duration of the eclipse phase of infected cells to be one day [10] and also the mean productive-phase duration to be one day [29]. Measurements of the lifetime virion production (burst size) of an infected cell range from a few hundred to tens of thousands [18, 7]. As in previous modeling work [23] we'll use a mid-range burst size value of $B = 20000$ virions/cell which gives us a production rate $p = B\delta = 20000$ day^{-1}. We use a virion clearance rate of $c = 23$ day^{-1} [37]. While this value is for chronic infection, results of a clinical study suggest that clearance is just as fast during early HIV infection [53]. Estimates of the replication-competent fraction of virions in chronically infected individuals range from 10^{-3} to 10^{-4} [40, 30, 24] and there is evidence that this fraction is higher during the initial stages of infection [24]. We will take $Q_c = 10^{-3}$ as the fraction of competent viruses in the initial inoculum, and let $Q_a = 10^{-2}$ be the corresponding fraction of newly-produced viruses in the host. Drug efficacies are discussed in the text and are chosen in the range of $\varepsilon_{\mathrm{RTI}}, \varepsilon_{\mathrm{PI}} = 0.9$.

Two key parameters in our model are the inoculum size N_0 and the rate of infection of target cells during early infection, kT. There are no clear estimates of these in the literature. Occupational exposure, for example, includes a range of accidental exposures, from needle sticks to blood splashes, from chronically infected patients whose viral loads may vary by orders of magnitude [4]. Since there is so much uncertainty, we will make the simple assumption that the inoculum sizes for occupational exposure are uniformly distributed between zero and $N_{\max}$. Values of the maximum inoculum size $N_{\max}$ are discussed in the Results.

There is also no reliable estimate of kT for early infection, and even chronic infection estimates are not definitive. Previous modelling studies of chronic infection would put the early kT in the range of $10^{-3} - 10^{-1}$/day for an estimate of $T = 10^6$cells/ml [35]. Most recently, Vaidya et al. presented some evidence that early kT may be higher than its chronic-infection counterpart for SIV [47], and in keeping with this information, Pearson et al. recently used a value of $kT \simeq 10$/day for early infection in their theoretical paper [34]. We will allow kT to be drawn from a distribution computed as follows.

Ribeiro et al. [38] estimated the basic reproduction number R_0 for acute HIV infection, during the phase of exponential viral increase in 47 patients. Starting from

that data,

1. we calculated the R_0 for the one- or two-compartment models and derived an expression for kT in terms of R_0. E.g. for the one compartment model, we have that $kT = c\delta R_0/(pQ_a - \delta)$.
2. We obtained a reasonably good fit of the resulting distribution of kT with a log-normal distribution. In what follows, we will describe this distribution using its median (kT_{median}) and 95th percentile kT_{95} (95% of patients have a kT *below* this value).

Fig. 2.2a shows this fit for the one-compartment model, assuming baseline replication-competent viral production rate $pQ_a = 200$.

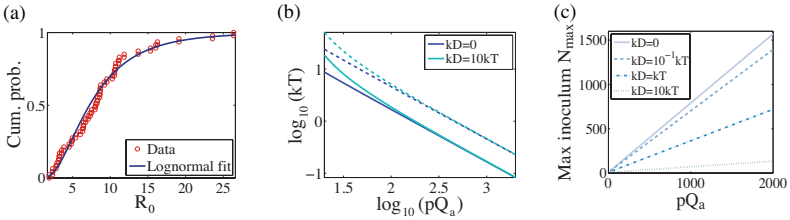

FIG. 2.2. ***Estimating infection rate*** kT ***and maximum inoculum size*** N_{max}. *(a) Log-normal fit of* kT *to the distribution of the basic reproduction number* R_0 *fits for early HIV infection from [38], as computed from the one-compartment model. (b) Distribution of* kT *for the one- (*$kD = 0$*) and two- (with* $kD = 10kT$*) compartment models illustrated by the median* kT_{median} *(solid) and 95th percentile* kT_{95} *(dashed) of the related log-normal distributions. Corresponding plots for* $kD \leq kT$ *would be practically indistinguishable from the* $kD = 0$ *plot. (c)* N_{max} *for a uniformly-distributed inoculum size, computed from the one- (*$kD = 0$*) and two- (*$kD \neq 0$*) compartment models, such that the risk of infection is fixed at 0.3%.*

In Fig. 2.2b we plot kT_{median} and kT_{95} for the one- and two- compartment models, for different values of pQ_a, to illustrate the predicted range in cell infection rates kT. In both case, the values of kT are in the range of estimates from previous work by other groups [47, 34]. For computations of risk discussed below, we will integrate over the full distribution of kT shown in Fig. 2.2a unless otherwise indicated.

In the two-compartment model, the blood and lymph compartments are connected by the action of dendritic cells. We estimate the transit time from the peripheral to lymph compartment to be $1/\rho = 2$ days and the lifetime of the DC in the lymph to be $1/\delta_D = 7$ days [27, 42]. Productively infected DCs have been found to produce less virus than T cells [51]. We estimate $B_D = 2000 = 10^{-1}B$ which is probably an overestimate, but allows us to consider a scenario where the action of DCs is emphasized. Finally, in the absence of better information we use the same values in both the periphery and lymph compartments for the remaining parameters. The exception is the infection rate of target cells kT_l which we take as a multiple of the peripheral rate kT, reflecting the increased density of CD4+ T cells and other targets in the lymphoid tissue.

Risk of infection. We now calculate the probability of becoming infected with HIV after exposure to a virus-only inoculum of size N_0 virions. The probability that there are n replication-competent virions in an inoculum of size N_0 is $\binom{N_0}{n} Q_c^n (1 - Q_c)^{N_0 - n}$, where Q_c is the fraction of replication-competent virions in the inoculum. Assuming that the viral lineages act independently and that a single replication-competent virion does *not* initiate HIV infection with probability q, the probabil-

ity of *clearing* the infection altogether is $\sum_{n=0}^{N_0} \binom{N_0}{n} Q_c^n (1-Q_c)^{N_0-n} q^n = (1 - Q_c(1-q))^{N_0}$. The overall risk of infection is then Risk $= 1 - (1 - Q_c(1-q))^{N_0}$. The parameter q depends on the infection rate kT, which we assumed to be log-normally distributed. Since we will assume that the inoculum size N_0 is uniformly distributed on $[0, N_{\max}]$, we can compute the mean risk of infection as Mean Risk $= \sum_{n=0}^{N_{max}} \frac{1}{N_{max}+1} \int_0^\infty [1 - (1 - Q_c(1 - q(kT)))^n] \, f(kT) \, dkT$ where $f(kT)$ is the log-normal probability density function over kT. Summing over n, we obtain

$$\text{Mean Risk} = 1 - \int_0^\infty \frac{1 - (1 - Q_c(1 - q(kT)))^{N_{max}+1}}{(N_{max}+1) Q_c (1 - q(kT))} f(kT) \, dkT. \tag{2.1}$$

Infection clearance probabilities. In order to calculate the mean risk of infection, we need to find q. The determination of q as a function of the model parameters for different possible models is the main focus of this paper. To start, we define multi-type continuous time branching process formulations for the models shown in Fig. 2.1 [21, 11, 9]. For the one-compartment model, define $P_{\tilde{m},\tilde{n},\tilde{v};m,n,v}(t,\tau)$ as the probability that at time t, $(T_1^*(t), T_2^*(t), V(t)) = (m,n,v)$ given that $(T_1^*(\tau), T_2^*(\tau), V(\tau)) = (\tilde{m},\tilde{n},\tilde{v})$ at some initial time τ. Note that W is a dead-end compartment that can be ignored in this calculation. In the following we will use $P_{\tilde{m},\tilde{n},\tilde{v}} := P_{\tilde{m},\tilde{n},\tilde{v};m,n,v}$ for notational convenience. From the master equation defining the model we can derive the corresponding backward Chapman-Kolmogorov differential equation [21]:

$$\begin{aligned}
\frac{dP_{\tilde{m},\tilde{n},\tilde{v}}}{d\tau} =& - s\tilde{m} P_{\tilde{m}-1,\tilde{n}+1,\tilde{v}} - \delta\tilde{n} P_{\tilde{m},\tilde{n}-1,\tilde{v}} - (1-\varepsilon_{\mathrm{PI}}(\tau)) Q_a p \tilde{n} P_{\tilde{m},\tilde{n},\tilde{v}+1} \\
& - c\tilde{v} P_{\tilde{m},\tilde{n},\tilde{v}-1} - (1-\varepsilon_{\mathrm{RTI}}(\tau)) kT \tilde{v} P_{\tilde{m}+1,\tilde{n},\tilde{v}-1} \\
& + [s\tilde{m} + (\delta + (1-\varepsilon_{\mathrm{PI}}(\tau)) Q_a p)\tilde{n} + (c + (1-\varepsilon_{\mathrm{RTI}}(\tau)) kT)\tilde{v}] \, P_{\tilde{m},\tilde{n},\tilde{v}}
\end{aligned} \tag{2.2}$$

with terminal condition $P_{\tilde{m},\tilde{n},\tilde{v};m,n,v}(t,t) = \delta_{m\tilde{m}}\delta_{n\tilde{n}}\delta_{v\tilde{v}}$. δ_{jk} is the Kronecker delta function. Note that this equation goes backwards in time, from $\tau = t$ to $\tau = 0$. Drug efficacies $\varepsilon_{\mathrm{RTI}}(\tau)$ and $\varepsilon_{\mathrm{PI}}(\tau)$ are time-dependent to capture the case of post-exposure prophylaxis where drugs are taken after exposure for a finite duration. Finally, q can be obtained as $q = \lim_{t\to\infty} P_{0,0,1;0,0,0}(t,0)$.

We analyze (2.2) using the probability generating function

$$\begin{aligned}
G_{\tilde{n},\tilde{m},\tilde{v}}(x,y,z;t,\tau) &= E\big[x^{T_1^*(t)} y^{T_2^*(t)} z^{V(t)} | T_1^*(\tau) = \tilde{n}, T_2^*(\tau) = \tilde{m}, V(\tau) = \tilde{v}\big] \\
&= \sum_{n,m,v=0}^{\infty} P_{\tilde{n},\tilde{m},\tilde{v};n,m,v}(t,\tau) x^n y^m z^v.
\end{aligned} \tag{2.3}$$

Note that $P_{0,0,1;0,0,0}(t,0) = G_{0,0,1}(0,0,0;t,0)$ so q can also be obtained as

$$q = \lim_{t\to\infty} G_{0,0,1}(0,0,0;t,0). \tag{2.4}$$

From (2.2) we can derive an infinite-dimensional system of differential equations for $G_{\tilde{n},\tilde{m},\tilde{v}}(x,y,z;t,\tau)$. This system can be reduced to three nonlinear equations by exploiting the branching property [21]: $G_{\tilde{n},\tilde{m},\tilde{v}} = (G_1)^{\tilde{n}} (G_2)^{\tilde{m}} (G_3)^{\tilde{v}}$, where $G_1 = G_{1,0,0}$,

$G_2 = G_{0,1,0}$, and $G_3 = G_{0,0,1}$. We obtain

$$\begin{aligned}\frac{\partial G_1}{\partial \tau} &= -s\,(G_2 - G_1)\\ \frac{\partial G_2}{\partial \tau} &= -\delta\,(1 - G_2) - (1 - \varepsilon_{\mathrm{PI}}(\tau))Q_a p G_2(G_3 - 1)\\ \frac{\partial G_3}{\partial \tau} &= -c\,(1 - G_3) - (1 - \varepsilon_{\mathrm{RTI}}(\tau))kT\,(G_1 - G_3)\end{aligned} \tag{2.5}$$

with terminal conditions $G_1|_{\tau=t} = x$, $G_2|_{\tau=t} = y$, and $G_3|_{\tau=t} = z$. To calculate the viral clearance probability, we need only solve (2.5) with terminal conditions $x = y = z = 0$ and compute the limit $q = \lim_{t\to\infty} P_{0,0,1;0,0,0}(t, 0)$. If the drug efficacy varies with time (as in the case of PEP), we solve this expression numerically. However, for no treatment or PrEP models, $\varepsilon_{\mathrm{RTI}}$ and $\varepsilon_{\mathrm{PI}}$ can be assumed constant and we can derive an analytic expression for q (see below).

Infection clearance probabilities under burst viral production assumption. If we instead assume that viral production occurs in a burst at infected cell death, the probability of clearing the infection assuming a single replication-competent virus for a given infection rate kT is slightly different than under the continuous viral production assumption as discussed in the previous section. We again derive the backward Chapman-Kolmogorov differential equation for the model, now under the burst viral production assumption:

$$\begin{aligned}\frac{dP_{\tilde{m},\tilde{n},\tilde{v}}}{d\tau} =& - s\tilde{m}P_{\tilde{m}-1,\tilde{n}+1,\tilde{v}} - \delta\tilde{n}P_{\tilde{m},\tilde{n}-1,\tilde{v}+(1-\varepsilon_{\mathrm{PI}}(\tau))Q_aB}\\ &- c\tilde{v}P_{\tilde{m},\tilde{n},\tilde{v}-1} - (1 - \varepsilon_{\mathrm{RTI}}(\tau))kT\tilde{v}P_{\tilde{m}+1,\tilde{n},\tilde{v}-1}\\ &+ (s\tilde{m} + \delta\tilde{n} + (c + (1 - \varepsilon_{\mathrm{RTI}}(\tau))kT)\tilde{v})\,P_{\tilde{m},\tilde{n},\tilde{v}}\end{aligned} \tag{2.6}$$

with terminal condition $P_{\tilde{m},\tilde{n},\tilde{v};m,n,v}(t, t) = \delta_{m\tilde{m}}\delta_{n\tilde{n}}\delta_{v\tilde{v}}$. The viral production term is no longer included. Rather, at cell death $(1 - \varepsilon_{\mathrm{PI}}(\tau))Q_aB$ virions are produced. This expression includes the simplification that the burst size is controlled by the drug efficacy at the moment of cell death, rather than including drug effects over the whole period of viral replication. In what follows, we will suppose that drug efficacy is either all-on or all-off, and thus the drug efficacy rarely changes during viral replication in an individual cell.

Defining the corresponding probability generating function

$$G(x, y, z; t, \tau) = \sum_{n,m,v=0}^{\infty} P_{\tilde{n},\tilde{m},\tilde{v};n,m,v}(t, \tau)x^n y^m z^v, \tag{2.7}$$

we derive the following equations:

$$\begin{aligned}\frac{\partial G_1}{\partial \tau} &= -s\,(G_2 - G_1)\\ \frac{\partial G_2}{\partial \tau} &= -\delta G_2 + \delta G_3^{(1-\varepsilon_{\mathrm{PI}}(\tau))Q_aB}\\ \frac{\partial G_3}{\partial \tau} &= -c\,(1 - G_3) - (1 - \varepsilon_{\mathrm{RTI}}(\tau))kT\,(G_1 - G_3)\end{aligned} \tag{2.8}$$

with terminal conditions $G_1|_{\tau=t} = x$, $G_2|_{\tau=t} = y$, and $G_3|_{\tau=t} = z$. Then we solve (2.8) with terminal conditions $x = y = z = 0$ and compute the limit, $q = \lim_{t\to\infty} G_3(0, 0, 0; t, 0)$.

Models with no treatment or PrEP. For constant $\varepsilon_{\mathrm{RTI}}$ and $\varepsilon_{\mathrm{PI}}$, the system (2.5) is autonomous. This allows us to reverse time and use the same system of equations going forward in time, with initial conditions $G_1|_{\tilde{t}=0} = x$, $G_2|_{\tilde{t}=0} = y$, and $G_3|_{\tilde{t}=0} = z$. The probability of extinction is then the G_3 coordinate of the stable fixed point of this system of equations. Performing the necessary computations, we find

$$q = \begin{cases} 1, & kT \leq \frac{c\delta}{pQ_a - \delta}, \\ \frac{\delta((1-\varepsilon_{\mathrm{RTI}})kT + c) + (1-\varepsilon_{\mathrm{PI}})cpQ_a}{(1-\varepsilon_{\mathrm{PI}})pQ_a((1-\varepsilon_{\mathrm{RTI}})kT + c)}, & kT > \frac{c\delta}{pQ_a - \delta}. \end{cases} \tag{2.9}$$

Note that, in the absence of drugs and assuming $Q_a = 1$, this is the same extinction probability obtained in [34], calculated using recursion relations. The inequalities involving kT are analogous to a basic reproductive number criterion in mathematical epidemiology, where for $R_0 \leq 1$ extinction is guaranteed ($q = 1$) while for $R_0 > 1$ infection is possible but not guaranteed ($0 < q < 1$).

Finally, combining (2.1) and (2.9) we can write down an integral formulation of mean risk of infection in terms of all model parameters. We will use this expression in estimating $N_{\max}$. In the case of burst production we find q as a root of a polynomial of order $(1 - \varepsilon_{\mathrm{PI}}(\tau))Q_aB$, which we calculate numerically.

3. Results.

3.1. Basic results on inoculum size, number of viral strains and model selection. Our first result is concerned with estimating a reasonable scale for the number of viruses in the initial inoculum. After that, we present a side-result of our model on the number of viruses from an inoculum that generate successful lineages within the host. This subsection of the results ends with some observations about the differences between the one- and two-compartment models. Further details on model selection (i.e. when to use the more complex model and when the two-compartment model is needed) are presented in detail in Appendix A. The main finding there is that the one-compartment model works well for looking at no treatment and PrEP.

Estimating inoculum size from the one-compartment model . A key parameter in our model is the inoculum size N_0. There is no clear estimate in the literature. For occupational exposure via needle accidents, one could estimate $\sim 0.1\mathrm{mm}^3 = 10^{-4}\mathrm{ml}$ of blood contact and then multiply by an estimate of the viral concentration in a chronically infected patient, $10^3 - 10^6/\mathrm{ml}$ [4] to obtain $N_0 \simeq 0.1 - 100$ virions, but for sexual exposure the calculation is much less clear.

As described in the Methods, we assume a uniform distribution of inoculum sizes. Then we can use our expression for mean infection risk (2.1) to obtain an estimate for the maximum value of $N_{\max}$ for a uniformly-distributed inoculum size N_0. The untreated per-act risk of infection following sexual or needlestick exposure has been estimated to be in the range of $0.1-1\%$ [26] in epidemiological studies. Using equation (2.1) and imposing a risk of 0.3%, we obtain Fig. 2.2c, which shows the maximum inoculum size $N_{\max}$ required to achieve a risk of infection of 0.3%, plotted against the replication-competent viral production rate pQ_a. In this figure we also vary the importance of dendritic cell translocation. We find a range of inoculum sizes on the order of $10^2 - 10^3$ across both models, with different assumptions about the DC infection rate kD. For our baseline value $pQ_a = 200\ \mathrm{day}^{-1}$ the range is the same as our simple estimation for needle accidents above, $O(10^2)$. Note that the required range in inoculum sizes decreases with DC uptake rate kD: if the rate is higher, a DC is more likely to be infected, and transport virus to the lymph. In what follows

we will fix other model parameters, and then compute the value of $N_{\max}$ required to produce an overall 0.3% risk of infection in the absence of treatment.

We observe that the combination of relatively small inoculum size and small fraction of replication-competent virus in the inoculum means that we are including many exposures that do not include any replication-competent virus. Further, we can estimate the number of founder virions in a successful infection. In agreement with recent reports [22], we find this number to be one with high probability, as discussed in the next paragraph.

Number of viral strains initiating HIV infection. Given an infection following exposure to N_0 virions, it is natural to ask how many virions actually initiate the infection, i.e. the number of founder strains. Clinical evidence shows this number to be quite small. For sexual exposure, a recent phylogenetic analysis of 102 patients showed that in 72 of them, the infection was initiated by a single virus [22]. We can use our model to predict the number of founder strains. Assuming each virion acts independently and that infection is successful, the probability of f founder strains is given by

$$P(F=f) = \frac{\sum_{n=0}^{N_0} \binom{N_0}{n} Q_c^n (1-Q_c)^{N_0-n} \binom{n}{f} (1-q)^f q^{n-f}}{1-(1-Q_c(1-q))^{N_0}}, \tag{3.1}$$

for q the probability of clearing a single virion as given by equation (2.9). Fig. 3.1 shows the probability of one to four founder strains for different inoculum sizes N_0 conditioned on successful infection. Our model predicts that with very high probability only a single virion initiates the infection. In retrospect this result makes sense: with a small per-exposure risk of infection [26], success of multiple independent lineages should be unlikely. This result suggests that infections initiated by multiple founder viruses may be caused by very severe exposures, multiple exposures, or some secondary transmission mechanism (e.g. infection in the presence of genital ulcerative diseases, in the case of sexual exposure).

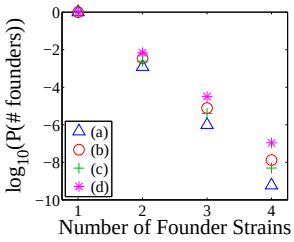

FIG. 3.1. $P(F=f)$ ***of*** f ***founder strains for different inoculum sizes*** N_0 ***and infection rates*** kT. *Using equation (3.1) we calculate the probability of* f *virions initiating the infection with the risk of successful infection fixed at* 0.3% *for median and maximum inoculum sizes* N_0 ($N_{max}/2$ *and* N_{max}, *respectively) and median and 95th percentile infection rates* kT (kT_{median} *and* kT_{95}, *respectively): (a)* $N_0 = N_{max}/2$, $kT = kT_{median}$, *(b)* $N_0 = N_{max}/2$, $kT = kT_{95}$, *(c)* $N_0 = N_{max}$, $kT = kT_{median}$, *(d)* $N_0 = N_{max}$, $kT = kT_{95}$. *Here,* $N_{max} = 148$, $kT_{median} = 0.84/day$ *and* $kT_{95} = 2.31/day$.

Impact of the two-compartment model on risk of infection. We now examine how the probability of infection changes between the one- and two-compartment models. We first calculate the distribution of kT so that the risk of infection using the one-compartment model is 0.3%. We then compute the probability of infection predicted by the two-compartment model for different values of kD and kT_l. Fig. 3.2 shows

this risk of infection as a function of the two-compartment model parameters kT_l/kT and kD/kT, for two different values of the dendritic cell burst size B_D. We observe

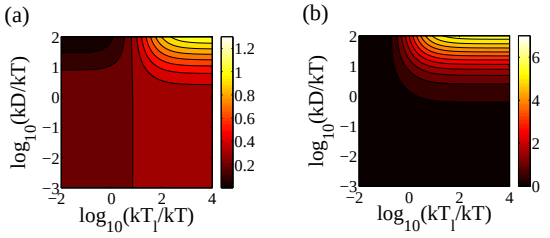

FIG. 3.2. ***Risk of infection from the two-compartment model compared to the simple, one-compartment model.*** *Colours and contours indicate the % risk of infection for varying DC infection rate kD and T cell infection rate in lymphoid tissue kT_l. (a) DC burst size $B_D = 10^{-3}B$; (b) $B_D = 10^{-1}B$. Note the colour axes are substantially different for the two panels.*

that the probability of infection is higher in the two-compartment model only if (i) the T cell infection rate in lymphoid tissue kT_l is comparable to or greater than kT, and (ii) the dendritic cell (DC) infection rate kD is comparable to or greater than kT. Fig. 3.2a also has the interesting feature that for the unlikely scenario of small kT_l and large kD the probability of infection is actually decreased by the addition of the second compartment. This is because with kD large, virions in the periphery preferentially infect DCs, but since kT_l is small, an ongoing infection in the lymphoid tissue is less likely. In this scenario, the lymphoid tissue acts as an unproductive sink habitat for virus.

While to our knowledge neither kD nor kT_l have been experimentally measured, it seems likely that kT_l is large compared to kT due to the high density of T cells in the lymphoid tissue. However, whether kD is large or small compared to kT is unclear: while the density of DCs is significantly less than the density of T cells [51], their surface receptors have been shown to have a relatively high affinity for HIV virions [41].

In studying inoculum size and PrEP, we found minimal differences between the predictions of our two models (see Appendix A) when all parameters were constant and the dynamics of viral extinction occur against a constant background. For PrEP, we therefore present results from the simpler, one-compartment model only. However, the efficacy of PEP is critically dependent on the treatment initiation delay after exposure, and the duration of treatment. For this reason, we found it important to use the two-compartment model which captures possible delays due to viral capture and transport by DCs, when studying PEP.

3.2. Risk reduction predictions for PrEP. In this subsection we will use the one-compartment model to predict the risk reduction achieved by taking ART in advance of exposure, as PrEP. We present basic risk-reduction estimates for reverse-transcriptase inhibitors (RTIs) and compare those with estimates for protease inhibitors (PIs). Unsurprisingly, however, we find that a combination of both drugs offers the greatest risk reduction, even if the drug efficacies are much lower than usually estimated.

Risk reduction estimates for PrEP with RTI drugs . Clinical studies so far have used reverse transcriptase inhibitors only [13, 2, 43, 48], so we begin by investigating risk reduction with RTIs only in our model. We compute relative risks of infection

from (2.1) and (2.9) assuming constant drug efficacy $\varepsilon_{\mathrm{RTI}}$. Fig. 3.3a shows risk reduction with increasing RTI efficacy, for different replication-competent viral production rates pQ_a. In each case the risk of infection in the absence of PrEP is 0.3%, and risk

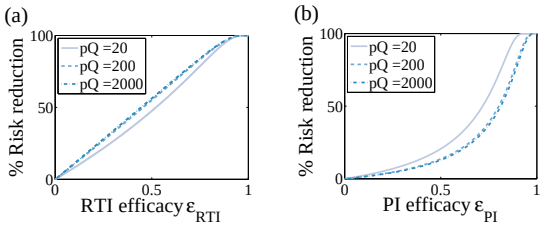

FIG. 3.3. ***Risk reduction for PrEP monotherapies.*** *We plot the percentage risk reduction for different replication-competent viral production rates pQ_a assuming (a) PrEP with RTI drugs only and (b) PI drugs only.*

reduction is computed relative to this benchmark (this means a 50% risk reduction corresponds to an actual risk of infection of 0.15%).

We observe substantial risk reductions even for moderate-efficacy drug treatments, across a range of likely replication-competent viral production rates pQ_a. Perhaps counter-intuitively, we find higher risk reductions for larger pQ_a. This is because a larger pQ_a leads to a lower estimate of the cellular infection rate kT in order to achieve the same fixed overall risk of infection in the absence of treatment (see Fig. 2.2).

Drug efficacies $\varepsilon_{\mathrm{RTI}}$, $\varepsilon_{\mathrm{PI}}$ are thought to be high, in the range of $0.9-1.0$ [20]. For such high values, we predict excellent risk reduction with PrEP for a wide range in the infection rate/inoculum size ($N_0 = 10 - 10^4$) and substantial risk reduction even if the efficacy is reduced, e.g. by less than perfect adherence to the drug regimen. Our estimates of risk reduction are high compared to the reduction obtained by clinical studies, but note that we are predicting a per-exposure risk. Repeated exposures could increase risk dramatically. Furthermore, we have assumed high drug adherence providing a constant drug efficacy *in situ* and a fixed background risk of 0.3%. Both assumptions may be violated in reality.

RTI drugs are preferable for single-drug PrEP. Fig. 3.3b shows the predicted risk reduction in the presence of protease inhibitors only, across different replication-competent viral production rates pQ_a. Comparing to panel (a), for equal drug efficacies, we see that RTIs are predicted to be more effective as PrEP than PIs, suggesting that RTIs are the better choice for single-drug PrEP. This result makes sense, since RTIs are effective at preventing the infection of new target cells, while PIs reduce the replication-competent fraction of virions produced, gaining effect only when there are already a number of infected cells and infection is beginning to establish itself.

Combination therapy as PrEP. Combination therapies, combining RTIs with PIs, have shown to be incredibly effective at controlling chronic HIV infection [3], motivating us to consider their use as PrEP. Fig. 3.4 shows the % risk reduction with increasing RTI and PI efficacy, for replication-competent viral production rates $pQ_a = 200$ and 2000. Notice that the contour plots are slightly asymmetric, in agreement with the previous result that (at equal efficacy) RTIs are better than PIs for PrEP. Overall, and unsurprisingly, we predict greater risk reduction for lower individual RTI/PI efficacies, suggesting that a combination of the two drugs may be a good alternative for PrEP, especially if poor drug adherence or viral drug resistance was to limit the efficacy of individual drugs.

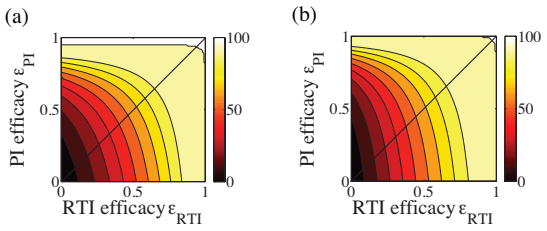

FIG. 3.4. ***Risk reduction for combination-therapy PrEP***. *Colours and contours indicate the percentage risk reduction for RTI+PI combination PrEP with (a) $pQ_a = 20$, (b) $pQ_a = 2000$. The diagonal line is drawn to indicate the asymmetry of the plots.*

3.3. Risk reduction predictions for PEP. We now examine post-exposure drug treatment as an intervention to prevent infection. In this section, the two-compartment model is used exclusively, in order to properly capture the effects of delays. We begin by showing our predictions of viral load dynamics over the first few days after exposure, with and without PEP, and then move on to estimating PEP efficacy under different treatment regimes. In each case, the possible effects of delayed treatment initiation and duration of therapy are highlighted. We then look at the sensitivity of the results to a number of key parameters in the model, specifically:

1. the delay before viral production in an infected cell (parameter s);
2. the possibility of reduced drug penetration to the lymph compartment;
3. the possibilities that DCs in the periphery are infected equally rapidly or more rapidly than other targets.

Viral load dynamics with PEP: increased probability of low viral load. To illustrate the effects of PEP in our two-compartment model, we examine the time evolution of viral load. Fig. 3.5 shows the probability distribution of the peripheral viral load in an individual over 3 days following exposure, with and without RTI-only PEP therapy. The plots show a slowly fattening tail (drawn on a log scale) corresponding to an increasing likelihood of fixation of infection. Here, we use the drug efficacy

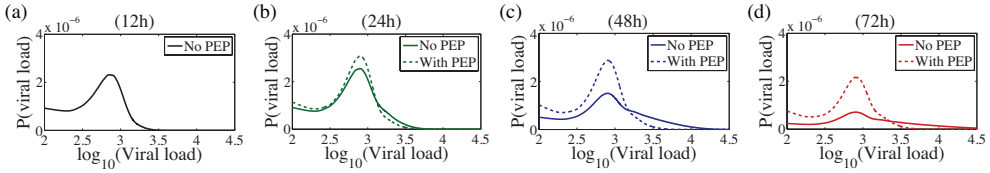

FIG. 3.5. ***Probability distributions of peripheral viral load*** $(V + W)$. *Predicted viral load distributions shown for (a) 12 hours, (b) 24 hours, (c) 48 hours, and (d) 72 hours after exposure, with and without PEP initiated at 12 hours. We assume RTIs only with efficacy $\varepsilon_{RTI} = 0.9$, inoculum size $N_0 = 10^2$ and we take $kD = 10^{-1}kT$ and $kT_l = 10^2 kT$.*

$\varepsilon_{\mathrm{RTI}} = 0.9$ and suppose that treatment is initiated 12 hours after exposure. This efficacy corresponds to the approximate average efficacy of azidothymidine (AZT) [25], the drug used in a 1997 meta-analysis of PEP for health care workers [6]. Today's drugs have higher efficacy. Our probability distribution curves were computed using probability generating functions rather than by extensive direct simulation; for details of our approach see [9]. We observe from these distributions that PEP increases the probability of lower viral load over time, increasing the probability of extinction - eventually.

Two weeks of single-drug PEP is predicted to be effective provided treatment is initiated promptly. Current recommendations for the timing and duration of PEP are based on animal studies from the 1990s using a single RTI (AZT) only [45, 6, 44]. The principle findings of these studies were that PEP for 28 days is effective but that 10- and 3-day regimens initiated 24 hours after exposure prevented infection only half the time, and not at all, respectively.

Fig. 3.6a shows the predicted risk reduction depending on treatment delay, for 1–4 week PEP monotherapy regimens. We assume that both possible drugs have a

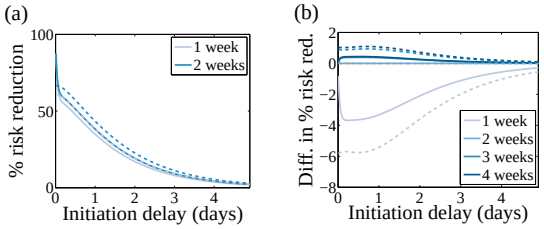

FIG. 3.6. ***Risk reduction with PEP as a function of delay in PEP initiation.*** *(a) We plot risk reduction given a regimen of 1 or 2 weeks, using RTIs only (solid lines) or PIs only (dashed lines). We fix the DC burst size $B_D = 2000$ virions, and drug efficacy equal to 0.9. (b) Difference in percentage risk reduction for 1-, 2-m 3- and 4-week regimens relative to the baseline of a 2-week regimen, with equal drug efficacy in all cell types and compartments.*

constant efficacy of 0.9. Our main observation here is that the treatment delay is the most important factor; treatment should begin with at most 2–3 days of exposure to give substantial risk reduction. In Fig. 3.6b we show the difference in percentage risk reduction between a baseline 2-week regimen, and regimens of lengths 1, 3 and 4 weeks. We observe that while the treatment duration is important, there is very little improvement predicted for regimens longer than 2 weeks. Additionally, when PEP is started within a few hours of the exposure time, RTIs are slightly preferable to PIs, in agreement with our PrEP results. However, for PEP initiated only after a few hours or later, we find that PIs are marginally more effective. The reason for this transition is that early initiation of RTIs suppresses infection of even a few cells. After that, keeping the replication-competent viral load low, as PIs do, more effectively enhances the probability that the infection will go extinct. This explanation is supported by the increased difference in risk reduction between PIs and RTIs over longer regimens (4 weeks vs 1 week). An exception to this general rule is found in the (probably unlikely) case that $kD > kT$, that is, that free viruses are more likely to bind to or infect DCs than target cells in the periphery (see below).

Combination therapy as PEP. Current recommendations for PEP are for combination therapy [50], usually with a combination of 1-2 RTIs of different types and a single PI. The contour plots in Fig. 3.7 show the predicted risk reduction as a function of PEP initiation delay and duration with combination therapy assuming a median cell infection rate, $kT_{\text{median}} \approx 0.84$. We predict significantly improved risk reduction, seen by comparing Fig. 3.7c (combination therapy) to Fig. 3.7a and b (RTIs only and PIs only). The improvement is enough to allow a slightly longer delay in initiation. For example, 50-60% risk reduction is achieved by a 4-week PEP regimen with both drug classes, initiated 48 hours after exposure. For a similar reduction with RTIs or PIs alone, the 4-week regimen must be initiated within 24–36 hours. Further, our results on PEP duration hold, in that regimens lasting longer than approximately two weeks offer little improvement in risk reduction (Fig. 3.7d, integrated over the

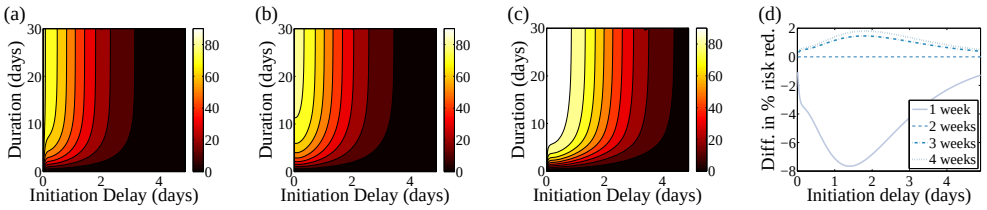

FIG. 3.7. ***Risk reduction with PEP as a function of delay in treatment initiation and duration.*** *Contours are set to 10% increments in risk reduction. We assume a DC burst size* $B_D = 2000$ *virions and constant drug efficacies of* 0.9. *(a) RTIs only; (b) PIs only; (c) combination therapy (RTIs and PIs). (d) The predicted change in risk reduction for 1-, 3- and 4-week combination therapy regimens relative to the (horizontal) baseline of a 2-week regimen.*

full distribution of cell infection rates kT).

PEP efficacy is fairly insensitive to eclipse phase duration assumption. The delay between infection of a cell and virion production (the eclipse phase duration) is expected to be an important factor in evaluating the impact of treatment initiation delay on PEP effectiveness. We therefore examined the impact of varying the eclipse phase duration ($1/s$). Our baseline assumption is that this phase lasts 1 day, the estimate for chronic infection [10]. Here, we consider also no eclipse phase or a mean 3-day eclipse phase. Fig. 3.8 shows the predicted change in risk reduction for 1- and 4-week PEP regimens relative to the baseline of a 2-week regimen (cf. Fig. 3.7d) for $s = \infty$ (no delay), 1, or $1/3$ day^{-1}. We note that as the mean eclipse phase duration is increased, predicted risk reduction is significantly improved under a 2-week regimen over a 1-week regimen, in particular under combination therapy (Fig. 3.8c). We also find that 4-week regimens are slightly more beneficial if a longer mean eclipse phase duration is assumed. However, the additional risk reduction offered by a 4-week regimen over a 2-week regimen remains on the order of 5% regardless of eclipse phase duration.

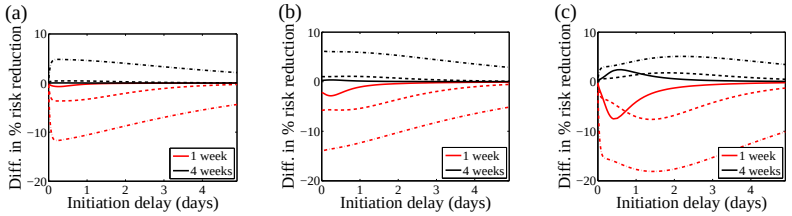

FIG. 3.8. ***Risk reduction with PEP as a function of delay in treatment initiation and duration under different eclipse phase duration assumptions.*** *The predicted change in risk reduction for 1- and 4-week regimens relative to the baseline of a 2-week RTI regimen, assuming a mean eclipse phase duration of 0 days (solid lines), 1 day (dashed lines), or 3 days (dash-dotted lines). We assume a DC burst size* $B_D = 2000$ *virions and constant drug efficacies* $\varepsilon_{RTI} = 0.9$ *and* $\varepsilon_{PI} = 0.9$, *once treatment starts. (a) RTIs only; (b) PIs only; (c) combination therapy (RTIs and PIs).*

Importance of PEP in halting DC-driven viral translocation. We also explore the effect of diminished drug efficacy in the DCs and the lymph for PEP, since again it is doubtful that drug penetration is equal in all tissues, or that efficacies are the same in all cell types [1]. Fig. 3.9b shows risk reductions assuming drug efficacies in the DCs are half that in the periphery/lymph ($\varepsilon^{(D)}_{\mathrm{RTI/PI}} = 0.5\varepsilon_{\mathrm{RTI/PI}}$), scaling selected for

illustration purposes only. We notice that, in comparison with Fig. 3.9a, the risk reductions are considerably smaller and the importance of early initiation of treatment is emphasized. Drug efficacies in lymph are halved instead in Fig. 3.9c ($\varepsilon_{\mathrm{RTI}}^{(D)} = \varepsilon_{\mathrm{RTI}}$, $\varepsilon_{\mathrm{RTI}}^{(L)} = 0.5\varepsilon_{\mathrm{RTI}}$). Comparison with Fig. 3.9a shows little difference in risk reduction. Taken together, the results of Fig. 3.9 emphasize the importance of DCs and in particular suggest that high drug efficacies in DCs are key to preventing initiation of infection, while drug efficacies in T cells in the lymph are of lesser importance. This is because once infection is carried to the lymph node by the DCs, infection takes off due to the higher density of target cells in the lymph, even for high drug efficacies.

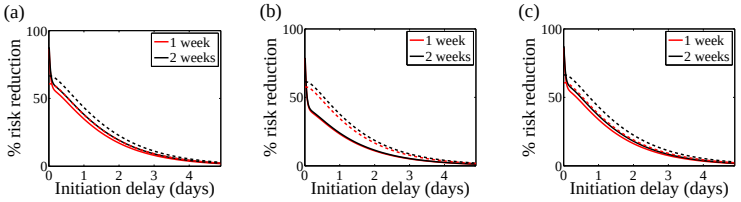

FIG. 3.9. **Risk reduction with PEP as a function of delay in PEP initiation**. *Risk reduction is plotted for a regimen of 1 or 2 weeks, using RTIs only (solid lines) or PIs only (dashed lines). We fix the DC burst size* $B_D = 2000$ *virions, and baseline peripheral drug efficacies* ε_{RTI} *and* ε_{PI} *of* 0.9. *(a) full drug efficacy in all cell types and compartments; (b) drug efficacies halved in DCs only; (c) drug efficacies halved in lymph only.*

Risk reduction predictions for PEP with $kD = kT$. We previously assumed that the DC infection rate kD is lower than the T cell infection rate in the periphery kT, based on the relative density of T cells and DCs. However, since surface DC receptors have been shown to have a relatively high affinity for HIV virions [41], whether kD is small or large relative to kT is unclear. We therefore repeat our PEP calculations with kD equal to or larger than kT : Fig. 3.10a-d shows risk reduction with PEP as a function of delay in treatment initiation and duration, assuming $kD = kT$. These are to be compared with results for $kD = 10^{-1}kT$ (Fig. 3.7). We observe that overall risk reduction is lessened for the same drug efficacy, since DCs are more likely to get infected and carry virus to the favourable habitat of the lymph. However, our qualitative prediction that month-long treatment regimens provide approximately the same risk reduction as a 2-week regimens, remains.

Risk reduction predictions for PEP with $kD > kT$. When we increase kD further to $kD = 10kT$, as in Fig. 3.10e-h, risk reduction predictions change more significantly. Comparing Figures 3.10a-d with 3.10e-h we observe that a PEP regimen of longer duration is required to achieve maximum possible risk reduction given an initiation delay. We also note that, assuming $kD = 10kT$, a longer delay (1-3 days) in PEP initiation allows roughly the same maximum risk reduction when compared to predictions for $kD = kT$. This result is sensible since in our model, DCs compete with T cells for virus in the periphery and given $kD = 10kT$, they out-compete T cells. Therefore the infection propagates mostly in the lymph, and this propagation is delayed relative to the time of exposure because the DCs must first travel to the lymph.

3.4. An alternative viral production model. Pearson et al. [34] showed that assumptions on viral production can strongly affect the probability of clearing the infection in branching process models. In this final subsection of the results, we investigate the impact of using the bursting viral production assumption (see Methods) on our predictions of PrEP and PEP efficacy. We begin by stating some

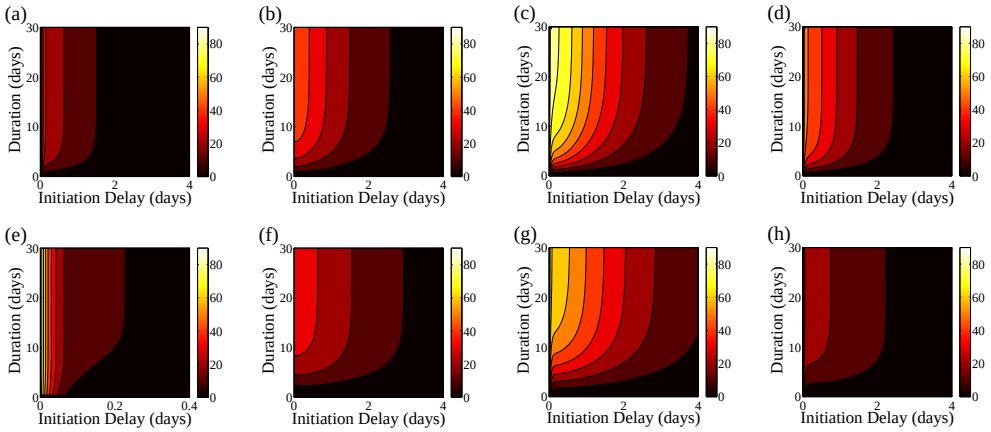

FIG. 3.10. **Risk reduction with PEP as a function of delay in treatment initiation and duration with reduced drug efficacy in lymph**. *Contours are set to 10% increments in risk reduction. We assume a DC burst size* $B_D = 2000$ *virions and full drug efficacies* $\varepsilon_{RTI} = 0.9$ *and* $\varepsilon_{PI} = 0.9$. *(a-d) with* $kD = kT$ *and (e-h)* $kD = 10kT$ *(a,e) RTIs only with full efficacy in all cell types and compartments. (b,f) PIs only with full efficacy in all cell types and compartments. (c,g) RTIs and PIs together with full efficacy in all cell types and compartments. (d,h) RTIs and PIs together with half efficacy in DCs, full efficacy elsewhere.*

simple properties of the bursting model. We then re-estimate the scale of the inoculum size and cellular infection rate, before showing that most of our results concerning PrEP and PEP remain qualitatively the same under this different model.

Number of virions produced under the different assumptions. We model burst viral production as the release of $B = p/\delta$ virions at cell death, so that the average number of virions released by a single cell is the same under both the continuous and burst viral production assumptions. However the probability distribution of the number of virions produced differs substantially: Under the burst assumption the number of virions released is $B = p/\delta$ with probability 1 while under the continuous production assumption, the distribution is $P(V = v) = \delta p^v/(\delta + p)^{v+1}$, shown in Fig. 3.11. The probability that the number of virions produced under the continuous production assumption is less than the mean B is $P(V < B) = \sum_{v=0}^{B-1} P(V = v) = 1 - (p/(\delta + p))^B \approx 0.63$. Therefore, under the continuous production assumption, a single infected cell will usually produce fewer virions. However, the variability is substantial and allows cells to occasionally produce a very high number of virions under the continuous production model. At low population numbers and equivalent parameters, these two effects significantly alter the extinction probability between the two models, and under burst production, the extinction probability is known to be lower (see extensive discussion by Pearson et al. [34]).

Estimating inoculum size and cell infection rate. We previously estimated distribution parameters for the infection rate kT (assuming a log-normal distribution) and the inoculum size N_0 (assuming a uniform distribution) for the continuous viral production assumption. Under the burst viral production assumption, the distribution parameters for kT are still computed from the basic reproduction number R_0, which is the same as under the continuous production assumption. Therefore the distribution parameters for kT are the same as presented in Fig. 2.2b. Fixing the risk of infection at 0.3% we can now compute the inoculum size for a range in the replication-competent burst size BQ_a, as shown in Fig. 3.12 for both continuous and

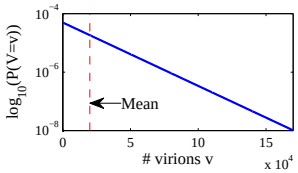

FIG. 3.11. **Probability distribution of number of virions produced by a single infected cell assuming continuous viral production**. *Note the log scale on the y−axis. The mean is equal to the number of virions produced under the burst viral production assumption.*

burst viral production assumptions. We can see that assuming burst viral production, a smaller inoculum size is enough to produce a fixed risk of infection, for a given kT. This is in agreement with the discussion above. However, the most important point is that the curves for the two production models (dashed vs solid lines) are not very different, and we can still conclude that the initial inoculum contains $O(10^2)$ virions. This prediction is fairly insensitive to kT for both production models, and is a consequence of the fixed overall probability of infection following exposure.

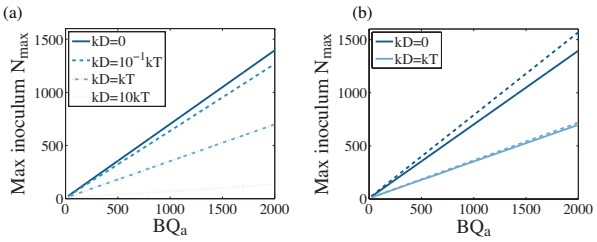

FIG. 3.12. **Estimating maximum inoculum size N_{max} under continuous and burst viral production assumptions**. *(a) N_{max} for a uniformly-distributed inoculum size is plotted against replication-competent burst size under the burst assumption, for different values of DC infection rate. (b) Comparison of N_{max} under continuous (solid) and bursting production (dashed) models for two values of DC infection rate. Both panels: curves are computed from the one- ($kD = 0$) and two- ($kD \neq 0$) compartment models, such that the risk of infection is fixed at 0.3%.*

PrEP effectiveness assuming burst viral production. Fig. 3.13ab shows model predictions of % risk reduction with PrEP assuming burst or continuous production of virions, using RTI and PI monotherapy, with drug efficacy 0.9 in all cell types and compartments. We observe qualitatively similar risk reductions with both drug classes under different viral production assumptions, with higher risk reduction in the case of continuous production. This is because the key mechanism in risk reduction is stopping the infection before it moves to the second generation of cells. In our model, the number of cells in the first generation (i.e. those infected by the initial inoculum) is usually very small, and the number of virions produced by those cells under the continuous production assumption is usually lower than the number produced under the burst assumption. The propagating infection is therefore more easily controlled. Thus RTIs and PIs offer better predicted risk reduction if we assume continuous viral production. However, the differences are small (less than 10 percentage points of risk reduction) and qualitative results remain: we find that predicted risk reductions with PrEP depend strongly on the initial inoculum size and cell infection rate kT. Again, for single-drug PrEP, RTIs should provide better protection than equally efficacious PIs.

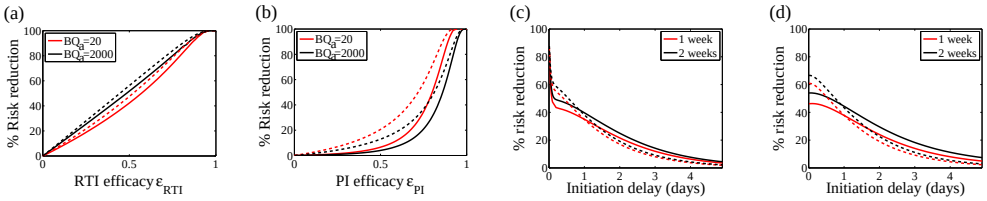

FIG. 3.13. **Risk reduction for PrEP and PEP monotherapies under different viral production assumptions**. *Reductions under burst and continuous viral production assumptions are indicated by solid and dashed lines respectively. (a,b) Percentage risk reduction for different replication-competent viral burst sizes BQ_a for PrEP with (a) RTI drugs only and (b) PI drugs only. (c,d) Percentage risk reduction as a function of delay in PEP initiation, given a regimen of 1 or 2 weeks for PEP with (a) RTI drugs only and (b) PI drugs only. We fix the DC burst size $B_D = 2000$ virions, and basic drug efficacies $\varepsilon_{RTI} = 0.9$ and $\varepsilon_{PI} = 0.9$, and assume drugs have equal efficacy in all cell types and compartments.*

PEP effectiveness under burst viral production. We also consider the effect of the viral production assumption on the predicted efficacy of PEP. Note that we now use a burst version of the two-compartment model, as in the main text. Fig. 3.13cd shows the percentage risk reduction induced by PEP regimens with either RTI or PI mono therapy, respectively, with drug efficacy 0.9 in all cell types and compartments, under either the burst or continuous production assumptions. For both drug classes we observe that the predicted reductions are qualitatively the same, but quantitatively slightly higher (after some delay) if we assume burst viral production. As with PrEP, we explain this through subtle differences in dynamics resulting from the viral production assumptions. PEP reduces risk of infection by keeping the viral load small, and hence enhancing the probability of extinction. When the number of infected cells is big, stochastic effects become less important, and the two models become essentially equivalent. However, the infection rate we estimate for a given inoculum size is lower under the burst assumption. The ongoing infection is therefore more easily controlled under the burst viral production assumption. As a result, the predicted risk reductions with PEP are larger with burst production than with continuous production. Most importantly, however, the quantitative differences in predicted risk reduction under the two viral production models are not large (less than 10%), and the results are qualitatively similar. Our conclusions regarding PEP timing and duration, as described previously, remain the same.

4. Discussion.

Pre-exposure prophylaxis. Recent PrEP trials have shown impressive reduction of incidence in at-risk populations [13, 2, 43, 48]. We predict that PrEP should be an effective prevention measure and that combination therapy should give some additional benefits in terms of improved risk reduction. This result was not affected by the choice of model (one vs two compartment) and was qualitatively insensitive to the exact values of parameters (not shown). One practical impediment to implementing combination therapy could be the cost of low adherence. Low adherence (30% of doses were missed) was reported in an earlier epidemiological study that did not determine a benefit of PrEP [36], and significant lack of adherence was also demonstrated in the recently ended FEM-PrEP study [48], which showed no positive results. Future modelling work should include variable drug adherence in an improved model of early infection. For a short, readable discussion of practical issues associated with PrEP, see Cohen and Baden (2012) [8].

Post-exposure prophylaxis. Current recommendations for PEP are based on limited animal studies from the 1990s that used RTI monotherapy only. Clinical guidelines based on these studies suggest that treatment should be initiated as soon as possible, no later than 3 days after exposure to HIV, and the duration should be approximately 1 month [26, 45, 6, 44, 5]. We predict that risk reduction falls to below 15% after a 3-day delay of treatment, regardless of duration, which is consistent with the guidelines. However, we generally predict little additional benefit from PEP regimens that exceed two weeks. This prediction is especially interesting in the context of PEP prescribed following risky behaviour, outside its application following occupational exposure to health care workers [5, 26], and in resource- limited settings. New investigations into shorter PEP durations would also be justified by the observation that PEP completion rates have been found to be quite low (varying from 24-78%, with adverse reactions given as the main reason for non-completion [5]). Furthermore, based on successful treatment of chronic infection, current guidelines recommend a combination of drugs as PEP. We find, unsurprisingly, that combination therapy can be expected to outperform monotherapy as PEP. Taken together, our results suggest that new experiments to analyze two-week PEP with a combination of drugs and a focus on non-occupational exposure could be worthwhile.

Drug resistance. It has been theorized that PrEP and PEP, especially with low adherence, could lead to the development of drug-resistant HIV. Drug resistance has not been reported as a consequence of either treatment, but it remains a significant concern. Although monitoring and perhaps experimental work in animal models will be essential to assess this risk, it also raises interesting modelling questions that can only be handled in a stochastic framework (since infection is a rare event, and a mutation to a drug-resistant strain during early infection with or without treatment will also be rare). In future work, we plan to build models for the development of drug resistance, and combine with an appropriate epidemiological model to study the likelihood of transmitted drug resistance in the context of PrEP use.

Developing models of HIV exposure. Our models are motivated by blood exposure to HIV, and are hence particularly applicable to occupational exposure. The mechanisms that lead to systemic infection after sexual exposure to HIV are likely more complicated. However, despite the simplicity of our models, our general framework may also be applicable to sexual exposure to HIV. High dose vaginal challenges of rhesus macaques have revealed that virus crosses the epithelial barrier to reach infectible cells within a few hours, allowing initial foci of 40-50 infected cells to become established, before involvement of dendritic cells, recruitment of further target cells, and eventual spread to the draining lymph nodes around one week after inoculation [33, 16, 17, 32]. Once the initial foci of infected cells at the exposure site become large enough and start to spread to the lymph, the probability of viral extinction is practically zero, regardless of whether the viral load has reached detection level in the peripheral blood or not.

With more experimental data, our model could be re-parametrized to capture these essential stages (local expansion followed by lymph involvement) for sexual exposure. Alternatively, in the case of blood exposure to HIV, it could be the case that peripheral viral replication does not usually occur, and so the key determinant of infection is whether the virus begins to replicate in the lymph nodes or another target-cell rich region. Under this assumption, our two-compartment model could be reduced to just the lymph compartment with an appropriate distribution on the initial number of viruses that reach the lymph. In this paper we briefly looked at

the parameter regime of the two-compartment model where peripheral virus is much more likely to be taken up by dendritic cells (and then taken to the lymph) than to infect targets in the periphery, which could be considered as a variant of this model.

Overall, we think it is likely that future models with more biological realism will achieve similar results to those presented here on the efficacy of PrEP and PEP strategies. We note that there is little difference in the estimated risk of infection between sexual and occupational exposure [26, 14, 49] so many of the overall constraints on parameters would hold for different routes of exposure. Additionally, though we did not explicitly include interferons, anti-viral chemokines or the influx of additional target cells upon exposure to virus directly, we presented our results for a range of parameter values that would be affected by the innate immune system, and found that our general conclusions remain the same.

Outlook. We have presented new theoretical results on the early dynamics of HIV infection in the presence of treatment, finding insights into the early-time dynamics that would be difficult to obtain experimentally. We believe that new models of the onset of HIV infection should become more specific to sexual transmission as more insights into the anatomy, physiology, and nature of virus-host interactions at the mucosa become available [16]. In particular, it would be useful to get better estimates of the density and infection rate of different populations of target cells at or near the site of infection, and to develop a clearer *in vivo* picture of the relative importance ofthe *cis-* and *trans-* infection roles of DCs in early infection. Improved models of sexual transmission will be of great benefit in understanding how HIV vaccines succeed or fail in controlling infection during the first few hours to days [52]. We believe that models of the kind presented here will be a valuable tool in future studies.

Appendix A. Model selection.

In the main text we presented two models of early HIV infection, a two-compartment model and a simpler, one-compartment model. We claimed that model predictions for inoculum size and PrEP - that is, in the absence of treatment delays associated with PEP - differ significantly only if the dendritic cell (DC) infection/virion take-up rate kD is larger than the target cell infection rate kT. We supported this claim by showing the inoculum size predictions from both models (Fig. 2, main text) and comparing the risk of infection produced by both models (Fig. 4, main text). We therefore used the simpler and more tractable one-compartment model to investigate the use of PrEP. Here we further support that choice of models with a brief exploration of inoculum size and predictions on PrEP .

Estimating inoculum size and cell infection rate under different DC burst size assumptions. As discussed in the main text, two key parameters in our model are the inoculum size N_0 and the rate of infection of target cells, kT, for which there are no clear estimates. We used results from [38] on the basic reproduction number R_0 to derive parameters for a log-normal distribution of the infection rate kT (see below). Then we assumed a uniform distribution of the inoculum size N_0 and computed the maximum inoculum size $N_{\max}$, showing that extending the model to two compartments has only a small impact on $N_{\max}$ predictions (unless we take the extreme case $kD = 10kT$; cf. Fig. 2 in the main text). There we assumed that the mean number of virions produced in the DCs, B_D, was one tenth of the mean number produced in target cells. This assumption was based on the observed poor replicative capacity of DCs [51], but estimates are lacking. Therefore in Fig. A.1 we show infection rates and inoculum sizes for different values of B_D. Note that the infection rate, as shown

in Fig. A.1a, is unaffected: the basic reproduction number $R_0 = kT(BQ_a - 1 - \sigma)/c$ (assuming $kD = \sigma kT$) is independent of the DC burst size B_D. In Fig. A.1b we observe that the estimated inoculum sizes differ very little: for higher B_D the maximum inoculum size $N_{\max}$ is only a bit smaller. Further, the inoculum size estimates shown for the two-compartment model with varying B_D also differ by little from estimates using the one-compartment model. This result gives further support to our claim that predictions of inoculum size are not very sensitive to model choice (assuming $kD = 10^{-1}kT < kT$).

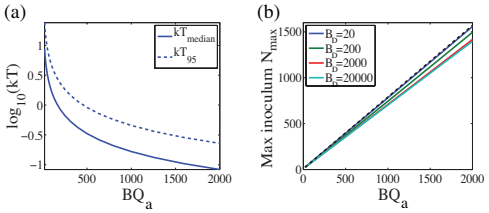

FIG. A.1. *Estimating inoculum size N_0 for the two-compartment model. (a) Range in kT for the two-compartment model assuming $kD = 10^{-1}kT$ as illustrated by the median of the related log-normal distributions for kT (solid line), and the 95th percentile value $kT = kT_{95}$ (dashed line). (b) We plot the maximum inoculum size N_{max}, under a uniform distribution assumption for inoculum sizes, for given replication-competent burst sizes BQ_a assuming the risk of successful infection fixed at 0.3% across different assumed total numbers of virions produced by the DCs, B_D. The black, dashed line corresponds to the inoculum size estimation in the one-compartment model, to be compared with Fig. 2 in the main text.*

PrEP predictions from the two-compartment model. Under the assumption that DC take-up/infectivity is less than the T cell infection rate, predictions regarding PrEP are also not very sensitive to model choice. Fig. A.2 shows % risk reduction for PrEP monotherapy regimens under different DC burst size assumptions, and predictions from the one-compartment model. Fig. A.2a,b shows risk reduction using RTIs only, Fig. A.2c,d using PIs only. We consider also the impact of diminished drug efficacy in the DCs and the lymph, since drug penetration and drug efficacies likely vary in different tissues and cell types, respectively [1]. In Fig. A.2a,c we assume drug efficacies are equal in all cell types and compartments, while in Fig. A.2b,d we assume half efficacy in the DCs, with normal efficacy elsewhere. In each case we observe similar qualitative results between the one- and two-compartment models even with different estimates of the DC burst size B_D. Further, quantitative differences - only notable in ranges of higher drug efficacy - remain relatively small. The important difference to note can be seen in Figures A.2b,d: when drug efficacies in DCs and lymph are halved (i.e. $\varepsilon_{\mathrm{RTI}}^{(D)} = \varepsilon_{\mathrm{RTI}}^{(L)} = 0.5\varepsilon_{\mathrm{RTI}}$), the risk reduction given effective drugs in the periphery is not 100%, as it is in the one-compartment model. In that case there is a non-zero probability that a DC takes up virus from the initial inoculum, and carries the infection to the lymph, where drugs are not assumed to completely inhibit viral replication. However, since this difference is less than 10%, and the qualitative similarities remain, we find that using the more tractable one-compartment model to make predictions about PrEP, for $kD < kT$, is sufficient.

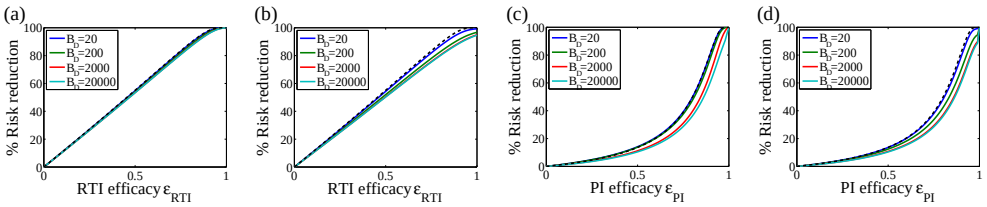

FIG. A.2. *Risk reduction for PrEP monotherapies for the two-compartment model. We plot the percentage risk reductions for different mean DC burst sizes B_D for (a,b) PrEP with RTIs only and (c,d) PrEP with PIs only. We assume drug efficacies in to be equal in all tissues/cell types in (a,c), and halved in the DCs and lymph compartments only in (b,d). The black, dashed line corresponds to the PrEP efficacy predictions from the one-compartment model.*

REFERENCES

[1] P.L. ANDERSON, J.J. KISER, E.M. GARDNER, J.E. ROWER, A. MEDITZ, AND R.M. GRANT, *Pharmacological considerations for tenofovir and emtricitabine to prevent HIV infection*, J Antimicrob Chemother, **66** (2011), pp. 240–250.

[2] J. M. BAETEN, D. DONNELL, P. NDASE, N. R. MUGO, J. D. CAMPBELL, J. WANGISI, J. W. TAPPERO, E. A. BUKUSI, C. R. COHEN, E. KATABIRA, A. RONALD, E. TUMWESIGYE, E. WERE, K. H. FIFE, J. KIARIE, C. FARQUHAR, G. JOHN-STEWART, A. KAKIA, J. ODOYO, A. MUCUNGUZI, E. NAKKU-JOLOBA, R. TWESIGYE, K. NGURE, C. APAKA, H. TAMOOH, F. GABONA, A. MUJUGIRA, D. PANTELEEFF, K. K. THOMAS, L. KIDOGUCHI, M. KROWS, J. REVALL, S. MORRISON, H. HAUGEN, M. EMMANUEL-OGIER, L. ONDREJCEK, R. W. COOMBS, L. FRENKEL, C. HENDRIX, N. N. BUMPUS, D. BANGSBERG, J. E. HABERER, W. S. STEVENS, J. R. LINGAPPA, C. CELUM, AND PARTNERS PREP STUDY TEAM, *Antiretroviral prophylaxis for HIV prevention in heterosexual men and women*, N Engl J Med, 367 (2012), pp. 399–410.

[3] J. A. BARTLETT, R. DEMASI, J. QUINN, C. MOXHAM, AND F. ROUSSEAU, *Overview of the effectiveness of triple combination therapy in antiretroviral-naive HIV-1 infected adults*, AIDS, **15** (2001), pp. 1369–1377.

[4] M. R. BETTS, D. R. AMBROZAK, D. C. DOUEK, S. BONHOEFFER, J. M. BRENCHLEY, J. P. CASAZZA, R. A. KOUP, AND L. J. PICKER, *Analysis of total human immunodeficiency virus (HIV)-specific CD4 and CD T-cell responses: relationship to viral load in untreated HIV infection*, J Virol, **75** (2001), pp. 11983–11991.

[5] J. BRYANT, L. BAXTER, AND S. HIRD, *Non-occupational postexposure prophylaxis for HIV: a systematic review*, Health Technol Assess, **13** (2009), pp. iii, ix–x, 1–60.

[6] D. M. CARDO, D. H. CULVER, C. A. CIESIELSKI, P. U. SRIVASTAVA, R. MARCUS, D. ABITEBOUL, J. HEPTONSTALL, G. IPPOLITO, F. LOT, P. MCKIBBEN, AND D. M. BELL, *A case-control study of HIV seroconversion in health care workers after percutaneous exposure*, New Engl J Med, **337** (1997), pp. 1485–1490.

[7] H.Y. CHEN, M.D. MASCIO, A.S. PERELSON, D.D. HO, AND L. ZHANG, *Determination of virus burst size in vivo using a single-cycle SIV in rhesus macaques*, Proc Natl Acad Sci USA, **104** (2007), pp. 19079–19084.

[8] M. S. COHEN AND L. R. BADEN, *Preexposure prophylaxis for HIV–where do we go from here?*, N Engl J Med, 367 (2012), pp. 459–61.

[9] J. M. CONWAY AND D. COOMBS, *A stochastic model for latently infected cell reactivation and viral blip generation in treated HIV patients*, PLoS Comput Biol, **7** (2011), p. e1002033.

[10] N.M. DIXIT, M. MARKOWITZ, D.D. HO, AND A.S. PERELSON, *Estimates of intracellular delay and average drug efficacy from viral load data of HIV-infected individuals under antiretroviral therapy*, Antiviral Therapy, **9** (2004), pp. 237–246.

[11] C.W. GARDINER, *Handbook of Stochastic Methods*, Springer-Verlag, 2004.

[12] D. T. GILLESPIE, *Exact stochastic simulation of coupled chemical reactions*, J. Phys. Chem., 81 (1977), pp. 2340–2361.

[13] R.M. GRANT, J.R. LAMA, P.L. ANDERSON, V. MCMAHAN, A.Y. LIU, L. VARGAS, P. GOICOCHEA, M. CASAPÍA, J.V. GUANIRA-CARRANZA, M.E. RAMIREZ-CARDICH, O. MONTOYA-HERRERA, T. FERNÁNDEZ, V.G. VELOSO, S.P. BUCHBINDER, S. CHARIYALERTSAK, M. SCHECHTER, L.-G. BEKKER, K.H. MAYER, E.G. KALLÁS, K.R. AMICO, K. MULLIGAN, L.R. BUSHMAN, R.J. HANCE, C. GANOZA, P. DEFECHEREUX, B. POSTLE, F. WANG,

J.J. McConnell, J.-H. Zheng, J. Lee, J.F. Rooney, H.S. Jaffe, A.I. Martinez, D.N Burns, D.V. Glidden, and the iPrEx Study Team, *Preexposure chemoprophylaxis for HIV prevention in men who have sex with men*, N Engl J Med, 363 (2010), pp. 2587–99.

[14] R. H. Gray, M. J. Wawer, R. Brookmeyer, N. K. Sewankambo, D. Serwadda, F. Wabwire-Mangen, T. Lutalo, X. B. Li, T. vanCott, and T. C. Quinn, *Probability of HIV-1 transmission per coital act in monogamous, heterosexual, HIV-1-discordant couples in Rakai, Uganda*, Lancet, **357** (2001), pp. 1149–1153.

[15] A. T. Haase, *Population biology of HIV-1 infection: Viral and CD4+ T cell demographics and dynamics in lymphatic tissues*, Annu Rev Immunol, **17** (1999), pp. 625–656.

[16] ———, *Targeting early infection to prevent HIV-1 mucosal transmission*, Nature, **464** (2010), pp. 217–223.

[17] ———, *Early events in sexual transmission of HIV and SIV and opportunities for interventions*, Annu Rev Immunol Rev Med, **62** (2011), pp. 127–139.

[18] A. T. Haase, K. Henry, M. Zupancic, G. Sedgewick, R.A. Faust, H. Melroe, W. Cavert, K. Gebhard, K. Staskus, Z.-Q. Zhang, P.J. Dailey, H.H. Balfour Jr., A. Erice, and A.S. Perelson, *Quantitative image analysis of HIV-1 infection in lymphoid tissue*, Science, (1996), pp. 985–989.

[19] J. M. Heffernan and L. M. Wahl, *Monte Carlo estimates of natural variation in HIV infection*, J Theor Biol, **236** (2005), pp. 137–153.

[20] B. L. Jilek, M. Zarr, M. E. Sampah, S. A. Rabi, C. K. Bullen, J. Lai, L. Shen, and R. F. F Siliciano, *A quantitative basis for antiretroviral therapy for HIV-1 infection*, Nat Med, 18 (2012), pp. 446–51.

[21] S. Karlin and H. M. Taylor, *A First Course in Stochastic Processes*, Academic Press, Inc, 1975.

[22] B. F. Keele, E. E. Giorgi, J. F. Salazar-Gonzalez, J. M. Decker, K. T. Pham, M. G. Salazar, C. X. Sun, T. Grayson, S. Y. Wang, H. Li, X. P. Wei, C. L. Jiang, J. L. Kirchherr, F. Gao, J. A. Anderson, L. H. Ping, R. Swanstrom, G. D. Tomaras, W. A. Blattner, P. A. Goepfert, J. M. Kilby, M. S. Saag, E. L. Delwart, M. P. Busch, M. S. Cohen, D. C. Montefiori, B. F. Haynes, B. Gaschen, G. S. Athreya, H. Y. Lee, N. Wood, C. Seoighe, A. S. Perelson, T. Bhattacharya, B. T. Korber, B. H. Hahn, and G. M. Shaw, *Identification and characterisation of transmitted and early founder virus envelopes in primary HIV-1 infection*, Proc Natl Acad Sci USA, **105** (2008), pp. 7552–7557.

[23] H.J. Kim and A. S. Perelson, *Viral and latent reservoir persistence in HIV-1-infected patients on therapy*, PLoS Comput Biol, **2** (2006), pp. 1232–1247.

[24] S. H. Kleinman, N. Lelie, and M. P. Busch, *Infectivity of human immunodeficiency virus-1, hepatitis C virus, and hepatitis B virus and risk of transmission by transfusion*, Transfusion, **49** (2009), pp. 2454–89.

[25] O. Krakovska and L.M. Wahl, *Optimal drug treatment regimens for HIV depend on adherence*, J Theor Biol, **246** (2007), pp. 499–509.

[26] R. J. Landovitz and J. S. Currier, *Postexposure prophylaxis for HIV infection*, New Engl J Med, **361** (2009), pp. 1768–1775.

[27] M.B. Lappin, J.M. Weiss, V. Delattre, B. Mai, H. Dittmar, C. Maier, K. Manke, S. Grabbe, S. Martin, and J.C. Simon, *Analysis of mouse dendritic cell migration in vivo upon subcutaneous and intravenous injection*, Immunology, **98** (1999), pp. 181–188.

[28] E. Le Corfec and H. C. Tuckwell, *Variability in early HIV-1 population dynamics*, AIDS, **12** (1998), pp. 960–962.

[29] M. Markowitz, M. Louie, A. Hurley, E. Sun, and M. Di Mascio, *A novel antiviral intervention results in more accurate assessment of human immunodeficiency virus type 1 replication dynamics and T-cell decay in vivo*, J Virol, **77** (2003), pp. 5037–5038.

[30] A. J. Marozsan, E. Fraundorf, A. Abraha, H. Baird, D. Moore, R. Troyer, I. Nankja, and E. J. Arts, *Relationships between infectious titer, capsid protein levels, and reverse transcriptase activities of diverse human immunodeficiency virus type 1 isolates*, J Virol, **78** (2004), pp. 11130–11141.

[31] S. J. Merrill, *The stochastic dance of early HIV infection*, J Comput Appl Math, **184** (2005), pp. 242–257.

[32] C. J. Miller, N. J. Alexander, S. Sutjipto, A. A. Lackner, A. Gettie, A. G. Hendrickx, L. J. Lowenstine, M. Jennings, and P. A. Marx, *Genital mucosal transmission of simian immunodeficiency virus - animal-model for heterosexual transmission of human immunodeficiency virus*, J Virol, **63** (1989), pp. 4277–4284.

[33] C. J. Miller, Q. S. Li, K. Abel, E. Y. Kim, Z. M. Ma, S. Wietgrefe, L. La Franco-Scheuch, L. Compton, L. J. Duan, M. D. Shore, M. Zupancic, M. Busch, J. Carlis,

S. Wolinksy, and A. T. Haase, *Propagation and dissemination of infection after vaginal transmission of simian immunodeficiency virus*, J Virol, **79** (2005), pp. 9217–9227.

[34] J.E. Pearson, P. Krapivsky, and A.S. Perelson, *Stochastic theory of early viral infection: Continuous versus burst production of virions*, PLoS Comput Biol, **7** (2011), p. e1001058.

[35] A.S. Perelson, Kirschner D.E., and R.J. De Boer, *Dynamics of HIV infection of CD4+ T cells*, Math Biosci, **114** (1993), p. 81.

[36] L. Peterson, D. Taylor, R. Roddy, G. Belai, P. Phillips, K. Nanda, R. Grant, E.E. Kekawo Clarke, A.S. Doh, R. Ridzon, H.S. Jaffe, and W. Cates, *Tenofovir Disoproxil Fumarate for prevention of HIV infection in women: A phase 2, double-blind, randomized, placebo-controlled trial*, PLoS Clin Trials, **2** (2007), p. e72.

[37] B. Ramratnam, S. Bonhoeffer, J. Binley, A. Hurley, and L.Q. Zhang, *Rapid production and clearance of HIV-1 and hepatitis C virus assessed by large volume plasma apheresis*, Lancet Infect Dis, **354** (1999), pp. 1782–1785.

[38] R. M. Ribeiro, L. Q. Qin, L. L. Chavez, D. Li, S. G. Self, and A. S. Perelson, *Estimation of the initial viral growth rate and basic reproductive number during acute HIV-1 infection*, J Virol, **84** (2010), pp. 6096–6102.

[39] M.E. Roland, T.B. Neilands, M.R. Krone, M.H. Katzl, K. Franses, R.M. Grant, M.P. Busch, F.M. Hecht, B.L. Shacklett, J.O. Kahn, J.D. Bamberger, T.J. Coates, M.A. Chesney, and J.N. Martin, *Seroconversion following nonoccupational postexposure prophylaxis against HIV*, Clin Infect Dis, **41** (2005), pp. 1507–1513.

[40] P. Rusert, M. Fischer, B. Joos, C. Leemann, H. Kuster, M. Flepp, S. Bonhoeffer, H. F. Gunthard, and A. Trkola, *Quantification of infectious HIV-1 plasma viral load using a boosted in vitro infection protocol*, Virology, **326** (2004), pp. 113–129.

[41] G.A. Snyder, J. Ford, P. Torabi-Parizi, Arthos. J.A., P. Schuck, M. Colonna, and P.D. Sun, *Characterization of DC-SIGN/R interaction with human immunodeficiency virus type 1 gp120 and ICAM molecules favors the receptor's role as an antigen-capturing rather than an adhesion receptor*, J Virol, **79** (2005), pp. 4589–98.

[42] L. Sompayrac, *How the Immune System Works*, Wiley-Blackwell, 2008.

[43] M. C. Thigpen, P. M. Kebaabetswe, L. A. Paxton, D. K. Smith, C. E. Rose, T. M. Segolodi, F. L. Henderson, S. R. Pathak, F. A. Soud, K. L. Chillag, R. Mutanhaurwa, L. I. Chirwa, M. Kasonde, D. Abebe, E. Buliva, R. J. Gvetadze, S. Johnson, T. Sukalac, V. T. Thomas, C. Hart, J. A. Johnson, C. K. Malotte, C. W. Hendrix, J. T. Brooks, and TDF2 Study Group, *Antiretroviral preexposure prophylaxis for heterosexual HIV transmission in Botswana*, N Engl J Med, 367 (2012), pp. 423–34.

[44] C. C. Tsai, P. Emau, K. E. Follis, T. W. Beck, R. E. Benveniste, N. Bischofberger, J. D. Lifson, and W. R. Morton, *Effectiveness of postinoculation (R)-9-(2-Phosphonylmethoxypropyl) adenine treatment for prevention of persistent simian immunodeficiency virus SIVmne infection depends critically on timing of initiation and duration of treatment*, J Virol, **72** (1998), pp. 4265–4273.

[45] C. C. Tsai, K. E. Follis, A. Sabo, T. W. Beck, R. F. Grant, N. Bischofberger, R. E. Benveniste, and R. Black, *Prevention of SIV infection in macaques by (R)-9-(2-Phosphonylmethoxypropyl)Adenine*, Science, **270** (1995), pp. 1197–1199.

[46] H. C. Tuckwell and E. Le Corfec, *A stochastic model for early HIV-1 population dynamics*, J Theor Biol, **195** (1998), pp. 451–463.

[47] N.K. Vaidya, R.M. Ribeiro, C.J. Miller, and A.S. Perelson, *Viral dynamics during primary simian immunodeficiency virus infection: Effect of time-dependent virus infectivity*, J Virol, **84** (2010), pp. 4302–4310.

[48] L. Van Damme, A. Corneli, K. Ahmed, K. Agot, J. Lombaard, S. Kapiga, M. Malahleha, F. Owino, R. Manongi, J. Onyango, L. Temu, M. C. Monedi, P. Mak'Oketch, M. Makanda, I. Reblin, S. E. Makatu, L. Saylor, H. Kiernan, S. Kirkendale, C. Wong, R. Grant, A. Kashuba, K. Nanda, J. Mandala, K. Fransen, J. Deese, T. Crucitti, T. D. Mastro, D. Taylor, and FEM-PrEP Study Group, *Preexposure prophylaxis for HIV infection among African women*, N Engl J Med, 367 (2012), pp. 411–22.

[49] M. J. Wawer, R. H. Gray, N. K. Sewankambo, D. Serwadda, X. B. Li, O. Laeyendecker, N. Kiwanuka, G. Kigozi, M. Kiddugavu, T. Lutalo, F. Nalugoda, F. Wabwire-Mangen, M. P. Meehan, and T. C. Quinn, *Rates of HIV-1 transmission per coital act, by stage of HIV-1 infection, in Rakai, Uganda*, J Infect Dis, **191** (2005), pp. 1403–1409.

[50] WHO HIV/AIDS Programme, *Post-Exposure Prophylaxis to Prevent HIV Infection: Joint WHO/ILO guidelines on post-exposure prophylaxis (PEP) to prevent HIV infection*, World Health Organization, 2007.

[51] L. Wu and V. N. KewalRamani, *Dendritic-cell interactions with HIV: infection and viral*

dissemination, Nat Rev Immunol, **6** (2006), pp. 859–868.

[52] A. J. Yates, M. Van Baalen, and R. Antia, *Virus replication strategies and the critical CTL numbers required for the control of infection*, PLoS Comput Biol, **7** (2011), p. e1002274.

[53] L. Zhang, R.M. Ribeiro, J.R. Mascola, M.G. Lewis, G. Stiegler, H. Katinger, A.S. Perelson, and M.P. Davenport, *Effects of antibody on viral kinetics in simian/human immunodeficiency virus infection: Implications for vaccination*, J Virol, **78** (2004), pp. 5520–5522.